I. Simulation Setup

A. Scenario/Layout

The data should ideally come from real-life measurements. However, measurements which include exhaustive beamsweep of all the links between UE and multiples gNBs are hard to obtain and are not currently available. We therefore opt for a ray-tracer based approach, which enables much larger volumes of data. The ray tracing is accurate in that it captures paths from all propagation phenomena like diffraction, reflections and transmissions. We use the commercial ray tracer from Remcom called Wireless Insite [1], which has been widely used in research communities [2], [3] and has been verified through mmWave measurements [4], [5]. This ray-tracing package has also been widely used in many ML experiments [6]–[9].

The first step in setting up the ray-tracer is to import the scenario layout. In our case, the scenario is downtown Rosslyn, Virginia[1]. The layout consists of building locations and dimensions in the area. The layout also includes materials from which these buildings are made so that the propagation mechanics like reflection, refraction and penetration of the scenario are accurately captured. Once the layout is imported into the ray-tracer, we place four gNBs (labeled BS in Fig. 1a) at some of the intersections in the city. The gNBs are approximately $200\,\mathrm{m}$ apart, translating to a cell radius of roughly $100\,\mathrm{m}$, which is consistent with the 3GPP Urban Micro "UMi" scenario [10]. These gNBs need to be assigned certain parameters like f_c, transmit bandwidth BW and other transmitter properties. The ray tracer also needs to consider the total number of paths i.e., the number of parts to consider from each gNB to each receiver point. We set this property equal to 20 in accordance with the 3GPP UMi NLOS scenario [10]. The ray tracer is configured to show the paths with a maximum of 2 reflections, 1 transmission and 0 diffractions. As described in [11], [12], mmWave systems will mostly rely on reflections for multi-path propagation, justifying the choice to mostly focus on reflections. Similarly, the 1 transmission means we only consider penetration of a signal through one obstacle[2]. The main mode of signal propagation in our work is line of sight (LOS) paths and non-line of sight (NLOS) reflected paths. The main sources of reflections are the buildings and terrain (ground). Once all the aforementioned parameters (listed in Table III) have been set, we place receiver points over

[1]This layout is also provided by Remcom inside Wireless Insite.

[2]Transmissions at mmWave are quite attenuated because of high penetration loss [13]. Hence, there is a very small chance that a signal transmitted through two different obstacles is received, so we only choose one transmission.

the entire layout grid spaced $0.5\,\mathrm{m}$ apart both in x and y axes. We deploy isotropic antennas at gNB and receiver points. Adding beamforming on top of these traces will be discussed in Section I-D. We now execute the ray-tracing. The ray-tracer output provides us with propagation information: (1) Received power on all the paths at each receiver point for each gNB, (2) The spatial information (e.g., path lengths, angle of arrivals and departures) of all these paths at each receiver point for each gNB and (3) The temporal information (i.e., delays) of all these paths at each receiver point for each gNB. All this information from the ray-tracer is sufficient to start modeling link quality (SNRs). In the next section, we discuss the addition of mobility to the current scenario.

B. Mobility

As mentioned above, the ray-tracer provides all the received signal information on the points in the layout grid (spaced $0.5\,\mathrm{m}$). The next step is to add mobility to the scenario. The goal is to mimic a vehicle (UE) moving downtown with velocity given in Table III (from [10]). We use the MATLAB Navigation Toolbox [14], which implements rapidly-exploring random tree (RRT) algorithm [15] to achieve this goal. MATLAB enables us to control various aspects of mobility: (a) Generating random routes for UEs, (b) Handling UE velocity in these routes and (c) Preventing collisions with obstacles (buildings) in these routes.

We start by importing the obstacle layout from the ray tracer to MATLAB. This layout is converted into *Binary Occupancy Grid* where length and width of each grid square is set to $0.5\,\mathrm{m}$. The binary occupancy grid assigns ones to the grid points where obstacles are present and zeros otherwise. At the beginning of each route, a starting point and an end point of the UE are sampled from the uniform distribution over the grid[3]. Similarly, a random velocity with distributions from Table III is assigned to the UE. To avoid collisions, we use the *Navigation Toolbox* [14] from MATLAB, which works on a binary occupancy grid and ensures that the UE does not collide with any buildings during the course of its route. The UE continues to move until a total of $T = 3000$ samples spaced $20\,\mathrm{ms}$ apart ($60\,\mathrm{s}$ for each trajectory, in accordance to the beam measurement periodicity from 3GPP [16]) are collected. We refer to these $T = 3000$

[3]It is ensured that the UE does not start inside any of the buildings (through a binary occupancy grid).

samples as a *trajectory*[4]. A total of 100 trajectories are generated. A generated trajectory with a binary occupancy grid is shown in Fig. 1b.

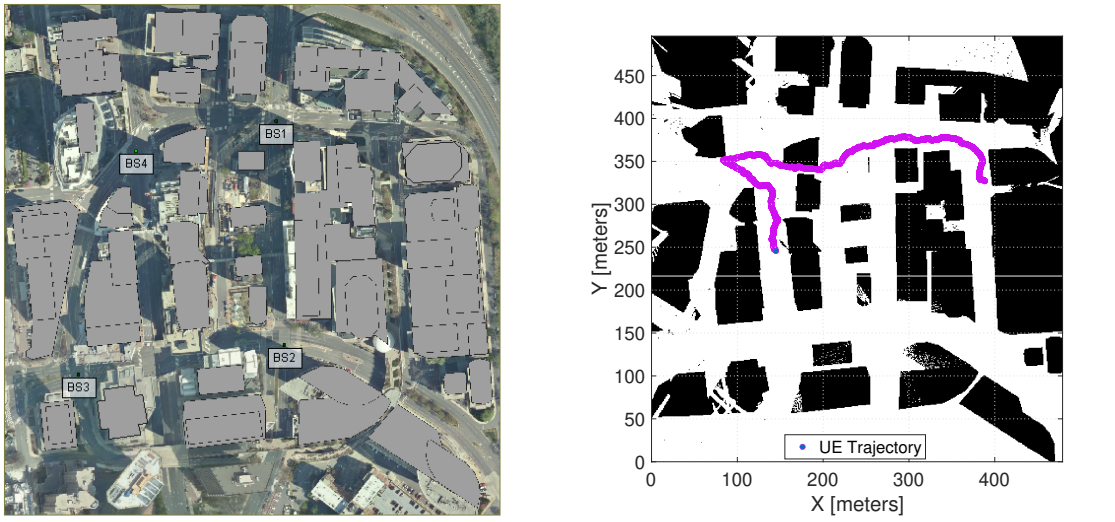

(a) Actual Layout of Downtown Rosslyn, VA

(b) Layout imported to MATLAB with UE Trajectory

Fig. 1: Demonstration of UE mobility in one of the trajectories in Downtown Rosslyn, VA

C. Hand Blockage Modeling

So far, the link quality generated from simulation trajectories captures the effect of multi-path, mobility and blockage by buildings. To make our simulations more realistic, we add the impact of hand blockage on link quality as well. Hand blockage is also something that has to be overcome in the mmWave regime. We use a linear interpolated hand blockage model from [17] based on measurements at $28\,\mathrm{GHz}$. The model depends on the angle of arrivals of different paths at the UE and the orientation of the UE (landscape or portrait). Since we use a ray tracer for our simulations, all the spatial information needed to implement the hand blockage model is available. For orientation, we choose one randomly at the start of each trajectory with equal probability. A hand blockage event on any path is triggered if the azimuth (elevation) angle of arrival $\zeta(\theta)$ falls in the range $[\zeta_1 \pm \upsilon/2]$ ($[\theta_1 \pm \kappa/2]$). The range signifies the azimuth (elevation)

[4]Multiple routes might be generated during the trajectory until the required number of samples are collected. Multiple routes are connected together by their end/start points i.e., the end point of the older route becomes the start point of the new route, ensuring continuity.

angular spread. Both azimuth and elevation angle of arrival conditions need to be true for a blockage event to be initiated. These conditions are similar to what has been proposed by the 3GPP standard to model hand blockage [10]. The values of ζ_1, υ, θ_1 and κ have been listed in Table I.

Orientation	ζ_1	υ	θ_1	κ	**Blockage Attenuation (A) (dB)**
Portrait mode	260^o	120^o	100^o	80^o	Weibull Distribution with $\alpha = 16.7$ and $\beta = 4.61$
Landscape mode	40^o	160^o	110^o	75^o	

TABLE I: Parameters for triggering hand blockage event

After triggering, the time dynamics of the blockage event are controlled by random variables τ_{d3dB}, τ_{r3dB} and τ_{Block}. Where τ_{D} is the total blockage event time , τ_{d3dB} and τ_{r3dB} represent the time taken for the signal to decay or rise by $3\,\mathrm{dB}$, respectively. These values (in ms) are generated upon triggering a blockage event and are provided in Table II [17], where $\mathrm{Weibull}(\alpha, \beta)$ denotes a weibull random variable with a probability distribution function (PDF) $f_{\mathrm{Weibull}}(.)$ given by:

$$f_{\mathrm{Weibull}}(x|\alpha,\beta) = \frac{\beta}{\alpha}(\frac{x}{\alpha})^{\beta-1}\exp(-(x/\alpha)^{\beta}),\ x \geq 0.$$

Parameters		τ_{d3dB}	τ_{r3dB}	τ_{D}
Weibull model parameters	α	0.044	0.045	0.59
	β	2.07	1.76	6.32

TABLE II: Parameters to model time dynamics of a hand blockage event

The blockage event on a particular path is modeled based on the parameters above using linear interpolation. We now define some parameters that will aid in the aforementioned linear interpolation.

$$\tau_{\mathrm{decay,rise}} = \frac{A\tau_{\mathrm{d3dB,r3dB}}}{3}, \tag{1}$$

where τ_{decay} is the time needed for the signal level to decay to A dB from the initial signal level. τ_{rise} is the time needed to rise to the normal signal level from A dB. The 3 in the denominator is because the transition is measured every $3\,\mathrm{dB}$. The total time of blockage event is given by:

$$\tau_{\mathrm{Block}} = \max(\tau_{\mathrm{decay}} + \tau_{\mathrm{rise}}, \tau_D). \tag{2}$$

The time during which the signal level remains constant at A dB during a blockage interval τ_{constant} is given by:

$$\tau_{\mathrm{constant}} = \tau_{\mathrm{Block}} - (\tau_{\mathrm{decay}} + \tau_{\mathrm{rise}}). \tag{3}$$

We now have all the parameters required to represent the blockage event in time. The loss suffered by hand blockage $\rho(\tau)$ at time sample τ can be represented in the following piece-wise linear manner:

$$\rho(\tau) := \begin{cases} \frac{A}{\tau_{\text{decay}}}\tau, & 0 \leq \tau < \tau_{decay}, \\ A, & \tau_{\text{decay}} \leq \tau < \tau_{\text{decay}} + \tau_{\text{constant}}, \\ A - \frac{A}{\tau_{\text{rise}}}\tau, & \tau_{\text{decay}} + \tau_{\text{constant}} \leq \tau < \tau_{\text{decay}} + \tau_{\text{constant}} + \tau_{\text{rise}} = \tau_{\text{Block}}. \end{cases} \tag{4}$$

It should be noted that $A < 0$ since it measures loss. Fig. 2a shows a blockage event labeled with all the parameters mentioned above.

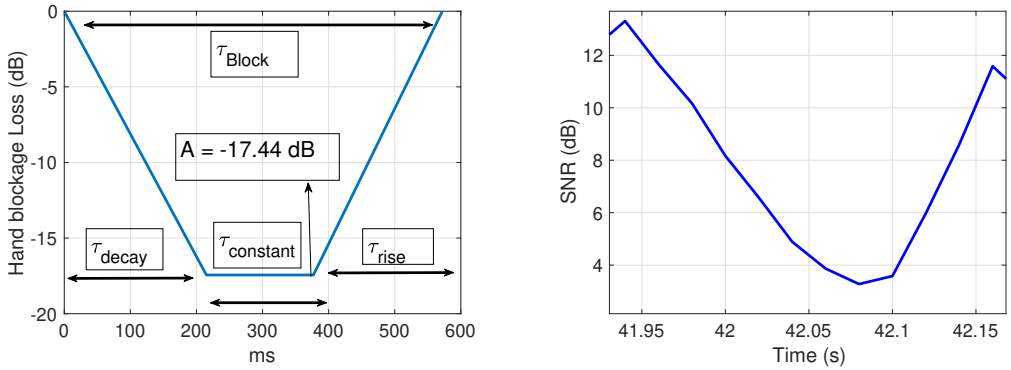

(a) Sample hand blockage event with labeled variables (b) Hand blockage event identified in one of the links from one of the trajectories

Fig. 2: Hand Blockage Model

D. Beamforming Codebook Design

A 4×2 uniform planar array (UPA) with $\lambda/2$ antenna spacing is assumed at the UE and an 8×8 UPA is assumed at the gNB. These sizes for $28\,\text{GHz}$ are similar to past capacity analyses such as [18]. We assume two identical antenna arrays at the UE and gNB for full 360 degree coverage, like practical devices [19] (i.e., one array covering the front hemisphere and the other covering the rear). Let $\mathcal{F}_j := \{\mathbf{f}_j^{(1)}, \mathbf{f}_j^{(2)}\}$ ($\mathcal{W}_l := \{\mathbf{w}_l^{(1)}, \mathbf{w}_l^{(2)}\}$) denote the pair of gNB (UE) beamforming vectors corresponding to the j-th (l-th) TX (RX) direction, where $\mathbf{f}_j^{(1)}, \mathbf{f}_j^{(2)} \in \mathbb{C}^{N_{\text{TX}}}$ ($\mathbf{w}_l^{(1)}, \mathbf{w}_l^{(2)} \in \mathbb{C}^{N_{\text{RX}}}$), correspond to the front and rear antenna arrays, respectively. We consider a simple beamforming codebook based on the steering vector of a UPA, such that the main lobes of the beam patterns cover the hemisphere, equally spaced in both azimuth and elevation. We refer the reader to [20] for the expressions of $\mathbf{f}_j^{(1)}, \mathbf{f}_j^{(2)}, \mathbf{w}_l^{(1)}$ and $\mathbf{w}_l^{(2)}$.

The antenna patterns for gNB and UE codebooks are shown in Fig. 3.

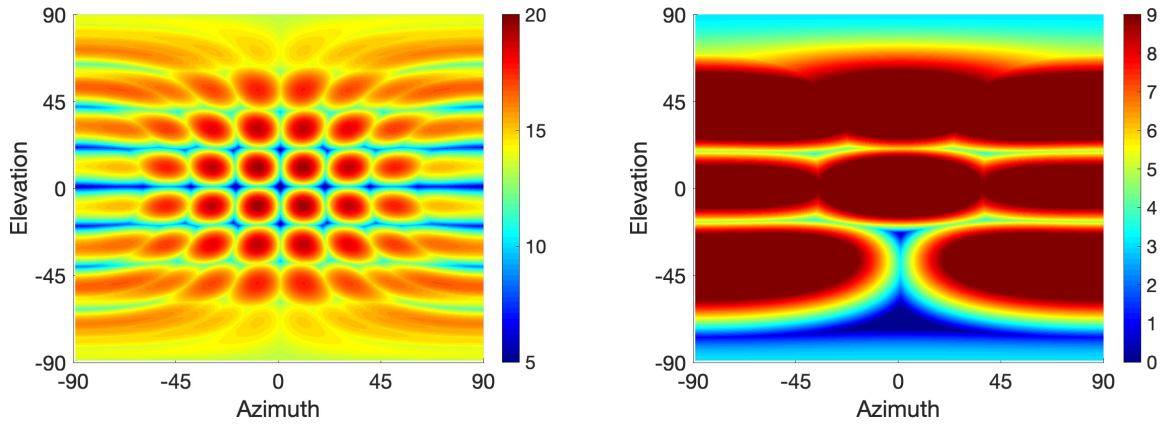

(a) gNB Codebook Design

(b) UE Codebook Design

Fig. 3: Antenna patterns associated with the designed codebook at gNB and UE

Parameters	**Value**	**Parameters**	**Value**	**Parameters**	**Value**
f_c	28 GHz	Bandwidth (‡)	400 MHz	N_{TX} (‡)	64
N_{RX} (‡)	8	N_{gNB} [21]	4	UE height (†)	1.7 m
gNB height (†)	10 m	Cell Radius [22]	$\sim$100 m	UE Velocity (†)	$\mathcal{U}$[0,27]m/s
Transmit Power [23]	23 dBm	Noise Figure [24]	9 dB	Sampling Interval [16]	20 ms
N_{Paths}	20	Number of Reflections	2	Number of Transmissions	0

TABLE III: Simulation parameters used for generating channel trajectories using ray-tracer. (†: [10], ‡: [25]). $\mathcal{U}[a,b]$ denotes a uniform random variable over $[a,b]$.

E. SNR Calculation

Given the rays for respective paths from the ray tracer for a trajectory n, we compute the wideband channel matrix for the i-th gNB, $\mathbf{H}_{i,n}(t,\nu)$, where ν denotes the frequency response argument. We apply the beamforming vectors to compute the SNR on each link. The expression for average wideband SNR $\gamma_n(i,j,l,t)$ is as follows:

$$\gamma_n(i,j,l,t) = 10\log_{10}\left(\max_{\substack{\mathbf{w}_l\in\mathcal{W}_l,\\ \mathbf{f}_j\in\mathcal{F}_j}} \int_{f_c-BW/2}^{f_c+BW/2} \frac{|\mathbf{w}_l^H \mathbf{H}_{i,n}(t,\nu)\mathbf{f}_j|^2}{k_{\mathrm{B}}(BW)N_F T_0} d\nu\right), \tag{5}$$

where k_{B} is Boltzmann's constant, BW denotes the system bandwidth, N_F the noise figure, and T_0 the temperature.

REFERENCES

[1] Remcom, "Wireless insite." [Online]. Available: http://www.remcom.com/wireless-insite

[2] A. Alkhateeb, S. Alex, P. Varkey, Y. Li, Q. Qu, and D. Tujkovic, "Deep learning coordinated beamforming for highly-mobile millimeter wave systems," *IEEE Access*, vol. 6, pp. 37 328–37 348, 2018.

[3] X. Yang and Y. Lu, "Propagation characteristics of millimeter wave in circular tunnels," in *2006 7th Intl. Symposium on Antennas, Propagation EM Theory*, 2006, pp. 1–5.

[4] Q. Li, H. Shirani-Mehr, T. Balercia, A. Papathanassiou, G. Wu, S. Sun, M. K. Samimi, and T. S. Rappaport, "Validation of a geometry-based statistical mmwave channel model using ray-tracing simulation," in *2015 IEEE 81st Vehicular Technol. Conf. (VTC Spring)*, pp. 1–5.

[5] S. Wu, S. Hur, K. Whang, and M. Nekovee, "Intra-cluster characteristics of 28 GHz wireless channel in urban micro street canyon," in *2016 IEEE GLOBECOM*, 2016, pp. 1–6.

[6] A. Alkhateeb, "DeepMIMO: A generic deep learning dataset for millimeter wave and massive MIMO applications," *arXiv preprint arXiv:1902.06435*, 2019.

[7] M. Alrabeiah and A. Alkhateeb, "Deep learning for mmwave beam and blockage prediction using sub-6 GHz channels," *IEEE Trans. on Commun.*, vol. 68, no. 9, pp. 5504–5518, 2020.

[8] M. Alrabeiah and A. Alkhateeb, "Deep learning for TDD and FDD massive MIMO: Mapping channels in space and frequency," in *2019 53rd Asilomar Conf. on Signals, Systems, and Computers*, 2019, pp. 1465–1470.

[9] A. Taha, M. Alrabeiah, and A. Alkhateeb, "Enabling large intelligent surfaces with compressive sensing and deep learning," *IEEE Access*, vol. 9, pp. 44 304–44 321, 2021.

[10] 3GPP, "TR 38.901, Study on Channel Model for Frequencies From 0.5 to 100 GHz (Release 15) document," Jun. 2018.

[11] J. Jarvelainen, K. Haneda, and A. Karttunen, "Indoor propagation channel simulations at 60 GHz using point cloud data," *IEEE Trans. on Antennas and Propagation*, vol. 64, pp. 4457–4467, 2016.

[12] S. Ju, S. Hashim Ali Shah, M. Affan Javed, J. Li, G. Palteru, J. Robin, Y. Xing, O. Kanhere, and T. Rappaport, "Scattering mechanisms and modeling for terahertz wireless communications," in *IEEE ICC 2019*, 05 2019, pp. 1–7.

[13] N. Al-Falahy and O. Alani, "Millimetre wave frequency band as a candidate spectrum for 5G network architecture: A survey," *Physical Commun.*, vol. 32, Nov 2018.

[14] MATLAB, "Navigation toolbox." [Online]. Available: https://in.mathworks.com/products/navigation.html

[15] S. M. LaValle and J. James J. Kuffner, "Randomized kinodynamic planning," *The Intl. J. of Robotics Research*, vol. 20, no. 5, pp. 378–400, 2001. [Online]. Available: https://doi.org/10.1177/02783640122067453

[16] M. Giordani, M. Polese, A. Roy, D. Castor, and M. Zorzi, "A tutorial on beam management for 3GPP NR at mmWave frequencies," *IEEE Commun. Surveys Tuts.*, Sep. 2018.

[17] V. Raghavan, L. Akhoondzadeh-Asl, V. Podshivalov, J. Hulten, M. A. Tassoudji, O. H. Koymen, A. Sampath, and J. Li, "Statistical blockage modeling and robustness of beamforming in millimeter-wave systems," *IEEE Trans. on Microwave Theory and Techniques*, vol. 67, no. 7, pp. 3010–3024, 2019.

[18] T. Bai, A. Alkhateeb, and R. W. Heath, "Coverage and capacity of millimeter-wave cellular networks," *IEEE Commun. Mag.*, vol. 52, no. 9, pp. 70–77, Sep. 2014.

[19] V. Raghavan, A. Partyka, A. Sampath, S. Subramanian, O. H. Koymen, K. Ravid, J. Cezanne, K. Mukkavilli, and J. Li, "Millimeter-wave MIMO prototype: Measurements and experimental results," *IEEE Commun. Mag.*, vol. 56, no. 1, pp. 202–209, Jan. 2018.

[20] S. H. A. Shah, S. Aditya, and S. Rangan, "Power-efficient beam tracking during connected mode DRX in mmWave and sub-THz systems," *preprint TechRxiv:13046447*, Oct 2020.

[21] 3GPP, “Requirements for support of radio resource management ,” 3GPP TS 38.133 Release 15), Jul. 2019.

[22] M. R. Akdeniz, Y. Liu, S. Rangan, and E. Erkip, “Millimeter wave picocellular system evaluation for urban deployments,” in *2013 IEEE Globecom Workshops (GC Wkshps)*, Dec. 2013, pp. 105–110.

[23] 3GPP, “TR 38.214,, NR - Physical layer procedures for data - (release 15) document,” Jun. 2018.

[24] ——, “TR 38.900, study on channel model for frequency spectrum above 6 GHz release,” Jun. 2018.

[25] P. Skrimponis, S. Dutta, M. Mezzavilla, S. Rangan, S. H. Mirfarshbafan, C. Studer, J. Buckwalter, and M. Rodwell, “Power consumption analysis for mobile mmwave and sub-THz receivers,” in *2020 IEEE 6G Wireless Summit*, Mar. 2020, pp. 1–5.